Extended Mode-Based Bandwidth Analysis for Asymmetric Near-Field Communication Systems

Youndo Tak and Sangwook Nam

Abstract—**An extended mode-based analysis for near-field coupled antennas is proposed. Based on this analysis, a method for estimating 3 dB bandwidth of near-field communication (NFC) systems with non-identical electrically small antennas is also proposed. The estimated results are in good agreement with the results from a full EM simulation.**

Index Terms—**Addition theorem, antenna equivalent circuit, bandwidth estimation, electrically small antenna, near-field communication (NFC), near-field coupling.**

I. Introduction

According to the Shannon-Hartley theorem, the capacity of a communication system is strongly related to the 3 dB bandwidth of the system. Hence, in order to estimate the performance of a communication system, the bandwidth analysis of the system is required.

When the near-fields of two antennas are overlapped, an efficient short-range communication system can be easily constructed, and the coupling of near-field coupled antennas can be estimated by the addition theorem [1]. Especially, when an electrically small antenna (ESA) is used, the analysis of the antenna coupling is particularly easy to calculate, because the ESA predominantly generates the TE_{10} or TM_{10} mode [2], [3].

Recently, based on the addition theorem, the method for estimating the 3 dB bandwidth of the near-field communication (NFC) system is proposed for the symmetrical case where the same small antennas are used for both the transmitting and receiving antennas [4]. In addition, it is shown that, by using the correction factor which is proposed for considering the impedance characteristics of the antenna, the estimation accuracy can be improved more than the method in [5].

However, in actual NFC applications, for example, the NFC-based e-health monitoring system which is mentioned in [6], the transmitter and receiver are placed in different circumstances, respectively. Therefore, the types or dimensions of the transmitting and receiving antennas may not be identical to each other, and thus the previously proposed method cannot be applied. Therefore, the extended coupling model for the asymmetric case, where different antennas are used for the transmitting and receiving antennas, respectively, needs to be proposed, and consequently, the mode-based bandwidth analysis has to be modified based on the proposed model.

II. Extended Coupling Analysis for Near-Field Coupled Antennas Based on the Addition Theorem

The power ratios of each spherical modes generated by the antenna vary according to the type of antenna and its physical dimensions [7]. When the ratio of the radiated power for each spherical mode to the total radiated power is known, the radiation resistance for each mode can be given as:

Manuscript received March 11, 2011; revised June 21, 2011; accepted July 28, 2011. Date of publication September 15, 2011; date of current version January 05, 2012. This work was supported by the Korean government (MEST) under a National Research Foundation of Korea (NRF) Grant (No. 2011-0001270).

The authors are with the School of Electrical Engineering and INMC, Seoul National University, Seoul 151-742, Korea (e-mail: ydtak76@gmail.com; snam@snu.ac.kr).

Color versions of one or more of the figures in this communication are available online at http://ieeexplore.ieee.org.

Digital Object Identifier 10.1109/TAP.2011.2167946

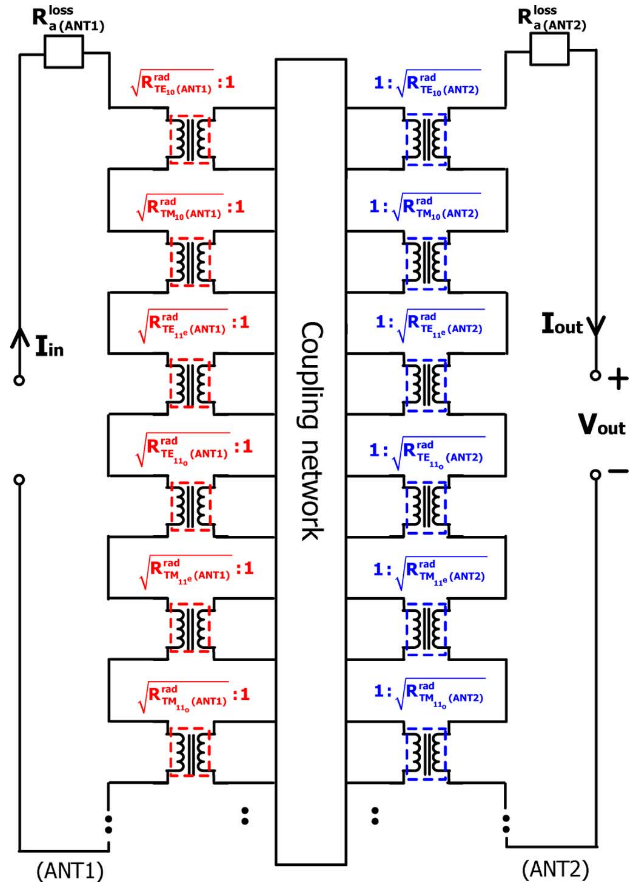

Fig. 1. Mode-based equivalent circuit for the coupled antennas of different characteristics.

$$R^{rad}_{TE_{nm^e_o}} = \frac{\mathrm{P}^{rad}_{TE_{nm^e_o}}}{\mathrm{P}^{rad}} R^{rad} \tag{1}$$

$$R^{rad}_{TM_{nm^e_o}} = \frac{\mathrm{P}^{rad}_{TM_{nm^e_o}}}{\mathrm{P}^{rad}} R^{rad} \tag{2}$$

where R^{rad} is the total radiation resistance, P^{rad} is the total radiation power, and $\mathrm{P}^{rad}_{TE_{nm^e_o}}$ and $\mathrm{P}^{rad}_{TM_{nm^e_o}}$ is the radiation power of the $TE_{nm^e_o}$ mode and the $TM_{nm^e_o}$ mode, respectively. In addition, when the input port of the antenna is matched, the coefficients of the normalized spherical mode functions are given by:

$$a_{TE_{nm^e_o}} = \sqrt{R^{rad}_{TE_{nm^e_o}}} I_{in} = \sqrt{R^{rad} \frac{\mathrm{P}^{rad}_{TE_{nm^e_o}}}{\mathrm{P}^{rad}}} I_{in} \tag{3}$$

$$a_{TM_{nm^e_o}} = \sqrt{R^{rad}_{TM_{nm^e_o}}} I_{in} = \sqrt{R^{rad} \frac{\mathrm{P}^{rad}_{TM_{nm^e_o}}}{\mathrm{P}^{rad}}} I_{in} \tag{4}$$

where I_{in} is the input current of the antenna, based on the definition of the generalized scattering parameters [2], [8].

If the transmitting and receiving antennas are designated as antenna 1 and antenna 2, respectively, and they are of different types or dimensions, the equivalent network for coupled antennas can be given as shown in Fig. 1, based on the network representation of the coupled antennas in [2]. In the network, each antenna is equivalently described as the transformer array, and the characteristics of each transformer are individually determined by the power ratios of spherical modes generated from each antenna.

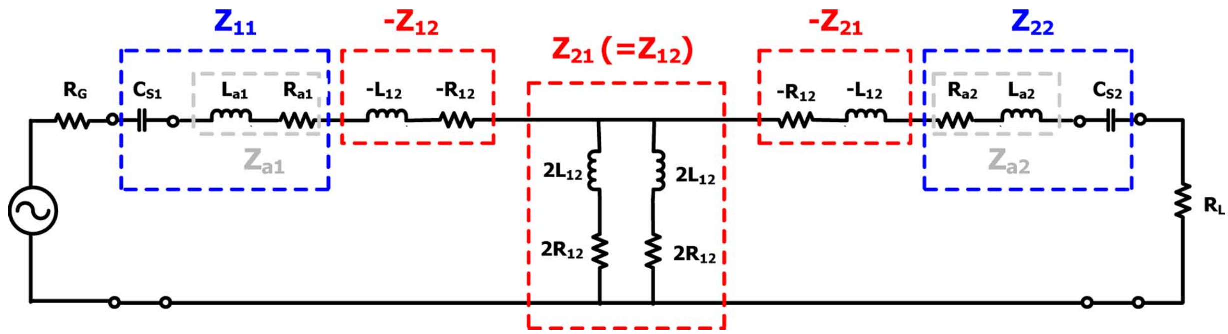

Fig. 2. Equivalent circuit description of coupled non-identical antennas.

Hence, the mutual impedance components of the coupling network between some spherical modes can be given as:

$$
\begin{aligned}
&Z_{21_{TE_{n'm'{}^{e}_{o}}TE_{nm^{e}_{o}}}} \\
&= \left.\frac{V_{TE_{n'm'{}^{e}_{o}}(ANT2)}}{I_{TE_{nm^{e}_{o}}(ANT1)}}\right|_{I_{out}=0} \\
&= \frac{\sqrt{R^{rad}_{TE_{n'm'{}^{e}_{o}}(ANT2)}}\left(a_{TE_{n'm'{}^{e}_{o}}(ANT2)}+a_{TE_{n'm'{}^{e}_{o}}(ANT2)}\right)}{\frac{1}{\sqrt{R^{rad}_{TE_{nm^{e}_{o}}(ANT1)}}}\left(a_{TE_{nm^{e}_{o}}(ANT1)}\right)} \\
&= \sqrt{R^{rad}_{TE_{nm^{e}_{o}}(ANT1)}}\sqrt{R^{rad}_{TE_{n'm'{}^{e}_{o}}(ANT2)}}A_{n'm'{}^{e}_{o}nm^{e}_{o}} \qquad (5)
\end{aligned}
$$

$$
\begin{aligned}
&Z_{21_{TE_{n'm'{}^{e}_{o}}TM_{nm^{e}_{o}}}} \\
&= \left.\frac{V_{TE_{n'm'{}^{e}_{o}}(ANT2)}}{I_{TM_{nm^{e}_{o}}(ANT1)}}\right|_{I_{out}=0} \\
&= \frac{\sqrt{R^{rad}_{TE_{n'm'{}^{e}_{o}}(ANT2)}}\left(a_{TE_{n'm'{}^{e}_{o}}(ANT2)}+a_{TE_{n'm'{}^{e}_{o}}(ANT2)}\right)}{\frac{1}{\sqrt{R^{rad}_{TM_{nm^{e}_{o}}(ANT1)}}}\left(a_{TM_{n'm'{}^{e}_{o}}(ANT1)}\right)} \\
&= \sqrt{R^{rad}_{TE_{n'm'{}^{e}_{o}}(ANT1)}}\sqrt{R^{rad}_{TM_{n'm'{}^{e}_{o}}(ANT2)}}B_{n'm'{}^{e}_{o}nm^{e}_{o}} \qquad (6)
\end{aligned}
$$

where the translation coefficients $A_{n'm'{}^{e}_{o}nm^{e}_{o}}$ and $B_{n'm'{}^{e}_{o}nm^{e}_{o}}$ are derived from the vector addition theorem [2], [9]. In addition, based on the duality of the electric field and the magnetic field, other parameters can be given as:

$$
\begin{aligned}
&Z_{21_{TM_{n'm'{}^{e}_{o}}TM_{nm^{e}_{o}}}} \\
&\quad= \sqrt{R^{rad}_{TM_{nm^{e}_{o}}(ANT1)}}\sqrt{R^{rad}_{TM_{n'm'{}^{e}_{o}}(ANT2)}}A_{n'm'{}^{e}_{o}nm^{e}_{o}} \qquad (7) \\
&Z_{21_{TM_{n'm'{}^{e}_{o}}TE_{nm^{e}_{o}}}} \\
&\quad= \sqrt{R^{rad}_{TM_{n'm'{}^{e}_{o}}(ANT1)}}\sqrt{R^{rad}_{TE_{n'm'{}^{e}_{o}}(ANT2)}}B_{n'm'{}^{e}_{o}nm^{e}_{o}}. \qquad (8)
\end{aligned}
$$

Since the input current is common for all ports of antenna 1, as shown in Fig. 1, the mutual impedance between coupled antennas can be given as:

$$
\begin{aligned}
Z_{21} &= \left.\frac{V_{out}}{I_{in}}\right|_{I_{out}=0} \\
&= \frac{\sum_{n',m'} V_{TE_{n'm'{}^{e}_{o}}(ANT2)} + \sum_{n',m'} V_{2_{TM_{n'm'{}^{e}_{o}}(ANT2)}}}{I_{in}} \\
&= \sum_{n,m,n',m'}\Big[Z_{21_{TE_{n'm'{}^{e}_{o}}TE_{nm^{e}_{o}}}} + Z_{21_{TM_{n'm'{}^{e}_{o}}TM_{nm^{e}_{o}}}} \\
&\quad + Z_{21_{TE_{n'm'{}^{e}_{o}}TM_{nm^{e}_{o}}}} + Z_{21_{TM_{n'm'{}^{e}_{o}}TE_{nm^{e}_{o}}}}\Big]. \qquad (9)
\end{aligned}
$$

III. Mode-Based Analysis of Bandwidth for the Near-Field Communication (NFC) System

In the previous study, the bandwidth analysis for the NFC comprised of symmetrical antennas is proposed by using the network analysis method for symmetrical 2-port networks based on the even-odd mode analysis [4]. However, when different antennas are used for transmitting and receiving antennas, respectively, the previously proposed analysis cannot be applied.

An NFC system with asymmetrical transmitting and receiving antenna can be generally described using the equivalent circuit shown in Fig. 2. In the equivalent circuit, the tuned transmitting antenna is represented as the circuit composed of R_{a1} and L_{a1}, which are the resistance and the reactance of the antenna itself, respectively, with the tuning capacitor C_{s1}. Similarly, the tuned receiving antenna is represented as the circuit composed of R_{a2}, L_{a2}, and C_{S2}. Because the transmitting antenna and the receiving antenna are different to each other, the components representing each antenna are differently given. In addition, the mutual impedance, which is reciprocal and composed of the real and imaginary components, is represented by L_{12} and R_{12}.

From the circuit theory, the transducer power gain of the two-port network can be given as:

$$G_T = \frac{4R_G R_L \left|Z_{21}\right|^2}{\left|(R_G+Z_{11})(R_L+Z_{22})-Z_{21}^2\right|^2} \qquad (10)$$

where the source impedance and the load impedance are given as R_G and R_L, respectively, and the mutual impedance is given as Z_{21} [10].

From (10), the characteristic equation to find the 3 dB fractional bandwidth can be given as:

$$a_4\left(\frac{2\Delta\omega_{3\text{ dB}}}{\omega_s}\right)^4 + a_2\left(\frac{2\Delta\omega_{3\text{ dB}}}{\omega_s}\right)^2 + a_1\left(\frac{2\Delta\omega_{3\text{ dB}}}{\omega_s}\right) + a_0 = 0 \qquad (11)$$

when the resonant frequency of the antenna is given as:

$$\omega_s = (L_{a1}C_{s1})^{-0.5} = (L_{a2}C_{s2})^{-0.5} \qquad (12)$$

and the coefficients of the equation are defined in Table I with additional parameters, defined as:

$$Q_{e1} = \frac{\omega_s L_{a1}}{R_G} = \frac{1}{\omega_s C_{s1} R_G} \qquad (13)$$

$$Q_{e2} = \frac{\omega_s L_{a2}}{R_L} = \frac{1}{\omega_s C_{s2} R_L} \qquad (14)$$

$$Q_{k1} = \frac{j\omega_s L_{12}}{R_G} \qquad (15)$$

and

$$Q_{k2} = \frac{j\omega_s L_{12}}{R_L} \qquad (16)$$

TABLE I
PARAMETERS FOR PROPOSED CHARACTERISTIC EQUATION.

Parameter	Expression
a_4	$\frac{Q_{e1}^2 Q_{e2}^2}{F_1^2 F_2^2}$
a_2	$\frac{2Q_{e1}Q_{e2}}{F_1F_2}\left(\frac{R_{12}R_{21}}{R_GR_L}-Q_{k1}Q_{k2}\right)+\frac{Q_{e1}^2}{F_1^2}\left(\frac{R_{a1}}{R_G}+1\right)^2+\frac{Q_{e2}^2}{F_2^2}\left(\frac{R_{a2}}{R_L}+1\right)^2$
a_1	$-2\left(\frac{R_{12}Q_{k1}}{R_L}+\frac{R_{21}Q_{k2}}{R_G}\right)\left\{\frac{Q_{e1}}{F_1}\left(\frac{R_{a2}}{R_L}+1\right)+\frac{Q_{e2}}{F_2}\left(\frac{R_{a1}}{R_G}+1\right)\right\}$
a_0	$2\left(\frac{R_{a1}}{R_G}+1\right)\left(\frac{R_{a2}}{R_L}+1\right)\left(\frac{R_{12}R_{21}}{R_GR_L}-Q_{k1}Q_{k2}\right)-\left(\frac{R_{a1}}{R_G}+1\right)^2\left(\frac{R_{a2}}{R_L}+1\right)^2+\left\{\left(\frac{R_{12}}{R_L}\right)^2+Q_{k2}^2\right\}\left\{\left(\frac{R_{21}}{R_G}\right)^2+Q_{k1}^2\right\}$

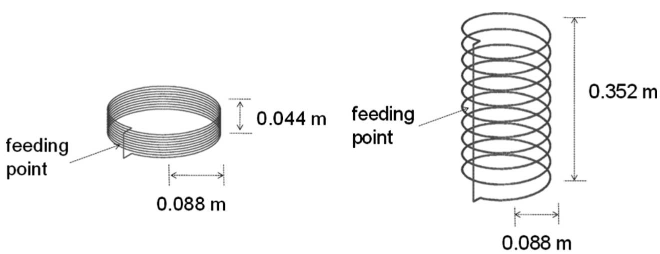

(a) (b)

Fig. 3. Solenoidal small antennas of different types (a) wide solenoidal small loop, and (b) narrow solenoidal small loop set to the receiving antenna.

under the condition that the correction factors are given as F_1 and F_2, respectively, in order to consider the actual impedance behavior of the antenna with respect to the frequency variations for each antenna, as proposed in [4].

IV. EXAMPLES

A. NFC Comprised of Different Solenoidal Antennas

As an example, the proposed method is applied to an NFC comprised of two 10-turn solenoidal small loop antennas of different types. According to the ratio of the radius to the height, the antennas are classified as wide and narrow types, as shown in Fig. 3. For the transmitting antenna, the wide solenoidal loop antenna is used, whereas the narrow solenoidal loop antenna is used for the receiving antenna. In addition, the operating frequency is set to 10 MHz, and the distance between the antennas is set to 0.5 m. The power ratios of the spherical mode are evaluated using the commercial EM software, FEKO, for each antenna, as shown in Table II.

B. NFC Comprised of a Helix Antenna and a Solenoidal Antenna

As another example, the proposed method is applied to an NFC comprised of one 10-turn open-ended helix, shown in Fig. 4(a), for the transmitting antenna, and a solenoidal small loop antenna, shown in Fig. 3(b), for the receiving antenna. The operating frequency is set to 20 MHz, and then the power ratios of the spherical mode are evaluated by the commercial EM software, as shown in Table III.

However, in contrast to the solenoidal loop, which can be equivalently described as a single parallel resonator, the open-ended helix cannot be approximated by a single parallel LC resonator, because the

TABLE II
POWER RATIO OF SPHERICAL MODES FOR THE SOLENOIDAL SMALL LOOP ANTENNAS AT 10 MHz

Wide Solenoidal Loop		Narrow Solenoidal Loop	
Modes	Power Ratio	Modes	Power Ratio
TE_{10}	91.77×10^{-2}	TE_{10}	60.86×10^{-2}
TM_{10}	8.1×10^{-2}	TM_{10}	37.87×10^{-2}
$TE_{1,\pm1}$	0.01×10^{-2}	$TE_{1,\pm1}$	0.61×10^{-2}
$TM_{1,\pm1}$	0.06×10^{-2}	$TM_{1,\pm1}$	0.02×10^{-2}

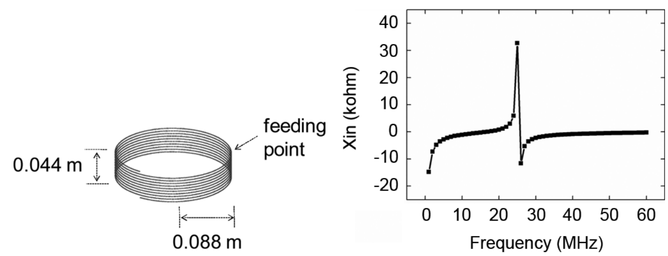

(a) (b)

Fig. 4. Wide open-ended small helix antenna (a) physical structure; (b) reactance behavior.

TABLE III
POWER RATIO OF SPHERICAL MODES FOR THE WIDE SMALL HELIX AND THE NARROW SOLENOIDAL SMALL LOOP ANTENNAS AT 20 MHz

Wide Helix		Narrow Solenoidal Loop	
Modes	Power Ratio	Modes	Power Ratio
TE_{10}	83.94×10^{-2}	TE_{10}	27.00×10^{-2}
TM_{10}	15.62×10^{-2}	TM_{10}	72.71×10^{-2}
$TE_{1,\pm1}$	0.00×10^{-2}	$TE_{1,\pm1}$	0.10×10^{-2}
$TM_{1,\pm1}$	0.22×10^{-2}	$TM_{1,\pm1}$	0.04×10^{-2}

reactance characteristic of the helix is given as shown in Fig. 4(b). According to the reactance behavior of the helix antenna with respect to the frequency variation, the antenna can be approximated to the equivalent circuit shown in Fig. 5. Hence, in order to consider the tuned open-ended helix as a simple RLC resonator circuit, its correction factor needs to be newly derived, as proposed in [4]. Based on the analysis proposed in [4], the correction factor can be defined as

$$F_2 = \left[\frac{1}{1-\left(\frac{\omega_s}{\omega_{ap}}\right)^2}+\frac{1}{\left(\frac{\omega_s}{\omega_{as}}\right)^2-1}\right]^{-1} \quad (17)$$

where the series resonant frequency of the antenna itself is given as ω_{as} and the parallel resonant frequency of the antenna itself is given as ω_{ap}.

C. Comparisons

The values of the 3 dB fractional bandwidth, which are calculated by the full EM simulation and the proposed method, are compared in Table IV. The configurations of the coupled antennas are classified into four cases according to the relative position and orientation of the antennas, as shown in Fig. 6. In addition, to be compared with other

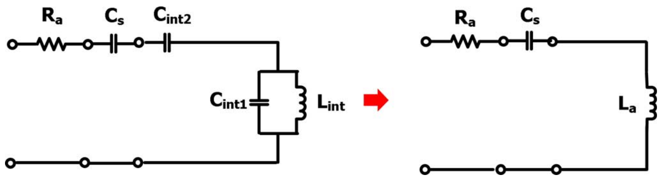

Fig. 5. Equivalent circuit representation of open-ended helix antenna.

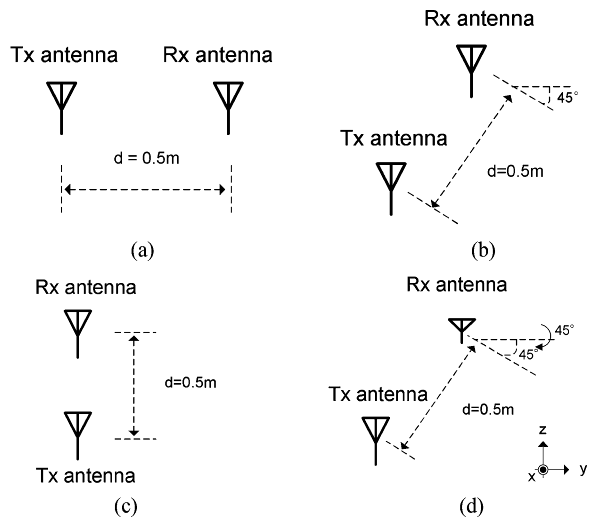

Fig. 6. Configurations of two coupled antennas (a) parallel configuration, (b) diagonal configuration, (c) collinear configuration, and (d) diagonal configuration with the receiving antenna $\pi/4$-rotated counter-clockwise about the positive y-axis.

TABLE IV
FRACTIONAL BANDWIDTH OF NEAR-FIELD COUPLED SMALL ANTENNAS

Antenna Type	Operating Frequency	Configuration	Fractional 3 dB BW ($\Delta\omega_{3dB}/\omega_s$)		
			EM Simulation	Proposed Method	
				Estimated FBW	Relative Error (to the EM Simulation)
Tx : WS Rx : NS	10MHz	Parallel	4.80×10^{-3}	4.89×10^{-3}	0.02
		Diagonal	4.00×10^{-3}	3.69×10^{-3}	-0.07
		Collinear	9.50×10^{-3}	8.44×10^{-3}	-0.11
		π/4-tilted diagonal	3.60×10^{-3}	3.45×10^{-3}	-0.04
Tx : WH Rx : NS	20MHz	Parallel	5.55×10^{-3}	5.38×10^{-3}	-0.02
		Diagonal	3.30×10^{-3}	3.34×10^{-3}	0.01
		Collinear	12.4×10^{-3}	11.0×10^{-3}	-0.11
		π/4-tilted diagonal	2.58×10^{-3}	2.61×10^{-3}	0.01

(WS: the wide solenoidal antenna, NS: the narrow solenoidal antenna, and WH: the wide open-ended helix)

work, the estimation results by the proposed method and the method presented in [5] are compared in Table V for the parallel configuration without rotation of receiving antenna.

The results shown in Table IV indicate that the 3 dB bandwidth of the NFC that uses non-identical antennas can be accurately estimated by the proposed method, which is based on the extended mode-based coupling model and the general equivalent description of the coupled antennas.

TABLE V
FRACTIONAL BANDWIDTH OF NEAR-FIELD COUPLED SMALL ANTENNAS IN PARALLEL CONFIGURATION

Type	Operating Frequency	Fractional 3-dB BW ($\Delta\omega_{3dB}/\omega_s$)			
		Proposed Method		Method in [5]	
		Estimated FBW	Relative Error (to the EM Simulation in Table IV)	Estimated FBW	Relative Error (to the EM Simulation in Table IV)
Tx : WS Rx : NS	10MHz	4.89×10^{-3}	0.02	5.65×10^{-3}	0.18
Tx : WH Rx : NS	20MHz	5.38×10^{-3}	-0.02	15.00×10^{-3}	1.70

(WS: the wide solenoidal antenna, NS: the narrow solenoidal antenna, and WH: the wide open-ended helix)

Additionally, from the results, it can be shown that the estimation errors for the collinear configuration are larger than others. They are thought to be due to the interaction between higher order modes, because the coupling between $\mathrm{TE}_{1,\pm1}$ and $\mathrm{TM}_{1,\pm1}$ is relatively large for the collinear configuration.

V. CONCLUSION

In this communication, an extended mode-based analysis of an NFC comprised of non-identical antennas is proposed. The coupling of antennas can be calculated using the addition theorem, and the bandwidth is analyzed based on the equivalent circuit description. The estimated values of the 3 dB bandwidth of the NFC are compared with EM simulation results. This comparison indicates that the bandwidth can be accurately estimated by the proposed method.

REFERENCES

[1] W. Wasylkiwskyj and W. K. Kahn, "Scattering properties and mutual coupling of antennas with prescribed radiation pattern," *IEEE Trans. Antennas Propag*, vol. 18, no. 6, pp. 741–752, 1970.

[2] J. Lee and S. Nam, "Fundamental aspects of near-field coupling antennas for wireless power transfer," *IEEE Trans. Antennas Propag*, vol. 58, no. 11, pp. 3442–3449, 2010.

[3] Y. Tak, J. Park, and S. Nam, "Mode-based analysis of resonant characteristics for near-field coupled small antennas," *IEEE Antennas Wireless Propag. Lett*, vol. 8, pp. 1238–1241, 2009.

[4] Y. Tak, J. Park, and S. Nam, "Mode-based estimation of 3 dB bandwidth for near-field communication systems," *IEEE Trans. Antennas Propag*, vol. 59, no. 8, pp. 3131–3135, 2011.

[5] H. C. Jing and Y. E. Wang, "Capacity performance of an inductively coupled near field communication system," presented at the IEEE Int. Symp. Antennas Propag, San Diego, CA, 2008.

[6] E. Strömmer, J. Kaartinen, J. Pärkkä, A. Ylisaukko-oja, and I. Korhonen, "Application of near field communication for health monitoring daily life," in *Proc. IEEE EMBS Annual Int. Conf.*, New York, 2006, pp. 3246–3249.

[7] Y. Tak, J. Park, and S. Nam, "The optimum operating frequency for near-field coupled small antennas," *IEEE Trans. Antennas Propag*, vol. 59, no. 3, pp. 1027–1031, 2011.

[8] D. M. Pozar, *Microwave Engineering*. New York: Wiley, 2005.

[9] W. C. Chew and Y. M. Wang, "Efficient ways to compute the vector addition theorem," *J. Electromagn. Waves Appl*, vol. 7, no. 5, pp. 651–665, 1993.

[10] J. O. Rollet, "Stability and power-gain invariants of linear two ports," *IRE Trans. Circuit Theory*, vol. 9, pp. 29–32, 1962.